Received: 20 December 2016 | Revised: 8 May 2017 | Accepted: 21 May 2017

DOI: 10.1002/pip.2907

WILEY

SHORT COMMUNICATION

A universal roll-to-roll slot-die coating approach towards high-efficiency organic photovoltaics

Yu-Ching Huang | Hou-Chin Cha | Charn-Ying Chen | Cheng-Si Tsao

Institute of Nuclear Energy Research, Longtan, Taoyaun 32546, Taiwan

Correspondence
Yu-Ching Huang, Institute of Nuclear Energy Research, Longtan, Taoyaun 32546, Taiwan.
Email: huangyc@iner.gov.tw

Abstract

This work develops a combinational use of solvent additive and in-line drying oven on the flexible organic photovoltaics to improve large-area roll-to-roll (R2R) slot-die coating process. Herein, addition of 1,8-diiodooctane (DIO) in the photoactive layer is conducted to yield a performance of 3.05% based on the blending of poly(3-hexylthiophene) (P3HT) and [6,6]-phenyl C_{61}-butyric acid methyl ester ($PC_{61}BM$), and a very promising device performance of 7.32% based on the blending of poly[[4,8-bis[(2-ethylhexyl)oxy] benzo[1,2-b:4,5-b'] dithiophene-2,6-diyl] [3-fluoro-2-[(2-ethylhexyl)carbonyl]thieno[3,4-b]thiophenediyl]] (PTB7) and [6,6]-phenyl C_{71}-butyric acid methyl ester ($PC_{71}BM$). Based on this R2R slot-die coating approach for various polymers, we demonstrate the high-performance result with respect to the up-scaling from small high-PCE cell to large-area module. This present study provides a route for fabricating a low-cost, large-area, and environmental-friendly flexible organic photovoltaics.

KEYWORDS

flexible, module, organic photovoltaics, roll-to-roll, slot-die

1 | INTRODUCTION

Organic photovoltaics (OPVs) exhibit many advantages of low cost, easy fabrication, and compatibility with flexible substrates. In addition, the scalability and remarkably low-energy payback time of OPVs is far superior to conventional inorganic photovoltaics.[1] Commercialization of OPVs has attracted a lot of attention because of the increasing power conversion efficiency (PCE) over 11%.[2,3] In contrast to the OPVs based on the well-known poly(3-hexylthiophene) (P3HT) polymer (PCE: 3 ~ 4%), the low-band-gap (LBG) polymer can significantly enhance the PCE (>7%). Many large-area solution-processing techniques, such as spray coating, inkjet printing, slot-die coating, doctor blade, and knife coating, are used to manufacture OPVs.[4-8] Among these techniques, slot-die coating is the most promising candidate for the applications of mass-production due to its high throughput, low material waste, low cost, and rapid manufacturing speed.[6-8] Recently, the highly efficient large-area–coated OPVs on glass and PET substrates have been reported in many literatures.[9-12] The current OPVs with high PCE were mainly fabricated by blade-coating technique, which is deemed to be a prototyping tool for slot-die coating and used for piece coating. Although the blade-coated OPVs show a comparable PCE (~9.5%) to the spin-coated OPVs,[11] the slot-die–coated OPVs on glass substrates still show a gap of performance with a PCE of only 5 ~ 6%.[7,13,14] Moreover, the performance of the flexible-substrate–based OPVs fabricated by roll-to-roll (R2R) slot-die coating process is limited to below ~5%[15,16] due to more challenges or inherent limitations from the special rolling process. There exist different mechanisms of film formation between blade-coating and R2R slot-die coating according to the literature,[17] leading to relatively little progress in the PCE improvement of flexible OPVs to date. To solve the critical problem regarding the R2R slot-die coating and film formation mechanism, we firstly propose the novel method combining the additive and drying oven temperature and demonstrate the remarkable improvement in the PCE of R2R flexible OPVs to 7.32%, which is far beyond the recent PCE record of ~5%. This breakthrough provides the feasible approach to make large progress toward commercialization of the R2R flexible OPVs, which is different from the general large-area sheet-to-sheet coating.

The active layer of OPVs usually exhibits a bulk heterojunction (BHJ) structure comprising electron donor (conjugated polymer) and electron acceptor (fullerene derivatives) phases.[18-20] The BHJ nanostructure of active layer has been shown to be a critical role in the overall PCE enhancement of OPVs. Several treatments have been developed to manipulate the BHJ structure of OPVs, such as thermal

Yu-Ching Huang and Hou-Chin Cha contributed equally to this work

annealing,[21] solvent annealing,[22] and solvent mixture,[23,24] to effectively improve PCE. Although these approaches can enhance the performance of OPVs, the treatment time usually takes more than the order of 10 minutes. These treatments would be limiting factors on the processing rate when they are applied to the continuous R2R printing facility. Therefore, a facile way to facilitate the processing rate is important to realize the printable OPVs technology. Recently, the application of solvent additives has been explored as an easy way to optimize the BHJ nanostructure of OPVs.[25] Variable solvent additives, such as 1-chloronaphthalene (CN),[26] nitrobenzene (NB),[27,28] and 1,8-diiodooctane (DIO),[29,30] have been introduced in high-performance OPVs, especially for LBG polymers. These solvent additives can effectively tailor the phase-separation behavior to form a favorable bicontinuous BHJ structure via their different solubility of the donor and acceptor materials.[31] For instance, in the most commonly used active layer system, poly(3-hexylthiophene) (P3HT) and [6,6]-phenyl C_{61}-butyric acid methyl ester ($PC_{61}BM$), DIO is a selectively better solvent for $PC_{61}BM$ than for P3HT, which would prevent from excessive $PC_{61}BM$ aggregation in the blend and also enhance the P3HT crystallization. In addition, DIO is the most-used solvent additive to enhance the PCE of devices based on LBG polymers, such as poly(thieno[3,4-b]thiophene-alt-benzodithiophene) (PTB7) and poly(2,6-(4,4-bis-(2-ethylhexyl)-4H-cyclopenta-[2,1-b;3,4-b']dithiophene) -*alt*-4,7(2,1,3-benzothiadiazole) (PCPDTBT). Previous literature[32] pointed out that the addition of DIO would facilitate dispersion of the PCBM molecules into the PTB7 polymer aggregates (or intercalation of PCBM molecules with polymer chains) and result in a favorable donor-acceptor interpenetration network. The additive can also adjust the evaporation time of host solvent for effectively increasing polymer crystallization. The use of solvent additives has shown a great improvement in PCE by controlling the BHJ morphology of OPVs at the multiple lengths, and different polymers are suitable for respective solvent additives. However, most of the additive-based devices were fabricated by conventionally laboratory-scale spin-coating process, which is not compatible with high-throughput R2R printing technique. The solvent evaporation behavior, film crystallization, and BHJ structure of the films formed by spin-coating process and R2R slot-die coating process are distinctively different. Establishing the fabrication technique of flexible R2R-coated OPVs cannot be directly transformed by the experience based on spin-coating process. This challenge motivates this study. On the other hand, PTB7 polymer is the model of the LBG polymers used for the spin-coated OPVs with high PCE.[33-35] However, to date, the influence of solvent additives on the morphology of R2R-coated OPVs reported elsewhere is based on the P3HT (PCE ~2%).[36,37] Recent literature reported that the R2R-coated flexible OPV based on PTB7-Th LBG polymer only exhibited a PCE of 2.42%.[38] These studies imply that the limited PCE improvement in the field of R2R-printed OPVs is still a bottleneck.

Understanding the relationship among the large-area–coating conditions, polymer materials, film morphology (phase-separated nanostructure), and performance is very important to develop R2R-coated flexible devices with high PCE. In our previous study,[17] we demonstrated that manipulation of the early-stage polymer crystallization during transformation of the wet film into solid-sate film in the R2R-coating process plays an important role in the performance improvement. In this study, we further illustrate how the BHJ film structure and performance of the R2R-coated P3HT:$PC_{61}BM$ OPV devices can be effectively improved by tuning the solvent additive contents and thermally processing condition. Furthermore, this technique was extended to the flexible R2R slot-die–coated PTB7/$PC_{71}BM$ active layer and finally achieved the PCE of 7.32%, which is, to the best of our knowledge, the highest PCE among the reported OPVs based on the R2R slot-die–coated fabrication and all LBG polymers. On the other hand, most of OPV studies adopted the halogenated solvents, such as chlorobenzene (CB) and 1,2-dichlorobenzene (DCB),[9,11,12] as the host solvent for LBG polymer. We further demonstrate that the R2R-coated OPVs with high PCE can be successfully fabricated in this study by using nonhalogenated solvent, o-xylene, as the host solvent. This study provides a solid basis of effective R2R slot-die coating route to achieve high-efficiency universally based on various polymers.

2 | EXPERIMENTAL

2.1 | Fabrication of R2R slot-die–coated inverted OPVs

We slot-die coated the electron transport layer (ETL) and photoactive layer by using Coatema R2R system (Coatema smartcoater, Germany). To obtain a flexible substrate suitable for use in the R2R system, we purchased the ITO-coated polyethylene terephthalate (PET) substrate with a surface resistance of 15 Ω/square from Optical Filters Ltd (EMI-ito 15). The PET/ITO substrate was firstly cut into a 10×10 cm^2 sheet, and then the substrate was treated with air plasma. Aluminum-doped zinc oxide (Al-ZnO, AZO) was used as the ELT in the present study, and the synthesis of AZO precursor and the slot-die coating parameters of AZO were described in our previous literature.[8,17] To obtain the P3HT:$PC_{61}BM$:DIO photoactive solution suitable for R2R slot-die process, 12-mg P3HT, 12-mg $PC_{61}BM$ (Rieke Metals), and various contents of DIO (Aldrich) were dissolved in 1-ml o-xylene solvent. For the PTB7:$PC_{71}BM$:DIO solution, we dissolved 6 mg of PTB7 (1-Mateirals), 9-mg $PC_{71}BM$ (Rieke Metals), and various contents of DIO in 1-ml o-xylene. These photoactive solutions were stirred at 50°C for overnight before slot-die coating. The slot-die coating layers were dried immediately by in-line oven equipped within the R2R-coating machine (R2R oven). To keep a stable R2R oven temperature, we preheated the oven at various temperatures for 40 minutes before coating. The slot-die coating speed used for ETL and photoactive layer was 1 m/min, and the input rates of ETL and photoactive layer were 0.8 and 1.2 ml/min, respectively. The deposited ETL was dried at 150°C for 10 minutes in an ambient oven, and the deposited wet photoactive layers were dried at various R2R oven temperature. To clarify the effect of DIO addition on the PCE of OPVs, we did not treat the photoactive layer with an additional thermal annealing process. The thicknesses of the slot-die–coated films of AZO, P3HT:$PC_{61}BM$:DIO, and PTB7:$PC_{71}BM$:DIO were about 60, 150, and 70 nm, respectively. To provide a hole transporting layer (HTL) and top metal electrode, we thermally evaporated MoO_3 (5 nm) and Ag (100 nm) films on the photoactive layer by using a shadow mask. The

devices used in this study were with the area of (1) 1 × 0.3 cm^2 and (2) 1 × 2 cm^2. Further, we also fabricated the module in the pattern comprising 20 cells in series and parallel connection (unit cell area: 1 × 1 cm^2). The configuration of connected cells in the module is based on the literature.[39] Figure 1 shows the structure of the devices and the module. It is noteworthy to mention that all the R2R-coating processes were conducted in air environment.

2.2 | Characterization

The current density-voltage characteristics of the devices and module were measured by a source meter (Keithley 2400) under AM 1.5G illumination (100 mW/cm^2) using a solar simulator (Abet technologies, Model #11000). The thicknesses of films were measured by a profilometer (Alpha Step D-100, KLA Tencor). Surface roughness and morphology of the blend films were analyzed by atomic force microscopy (AFM, Digital Instruments, Nanoscale III). All the slot-die–coated devices were not encapsulated and measured under ambient atmosphere.

3 | RESULTS AND DISCUSSION

Previous studies have demonstrated the effect of solvent additive (DIO) on the performance of OPVs, which were mainly fabricated by conventional spin-coating process at the laboratory scale. To date, there are very few publications reporting how the solvent additive affects the performance of the devices manufactured by the R2R process. It is a challenge to develop an easy R2R coating for achieving the high-performance OPV. Because of the continuous coating features, such as stress on substrate, fluid flow, and viscosity, of roll-to-roll process, the printed wet films must be controlled to be entirely dried before they entered into the roller. In usual, the addition of the solvent additive into the active layer would reduce the film drying speed due to its high boiling point and thus hinder the coating rate and the formation of well-BHJ structure of R2R process. For overcoming this hindrance, we firstly studied the relationship between the content of the solvent additive and the feasible parameters of R2R slot-die–coated process on the flexible substrate. For the blend of P3HT:PC_{61}BM as the model system, the added amounts of DIO are 0.25, 0.5, and 1 vol%. The R2R oven temperature was set at 110°C. Figure 2 shows the J-V curves of slot-die–coated devices (cell area: 1 × 0.3 cm^2) prepared with various additive contents and without additional thermal annealing. Table 1 lists the electric characteristics of the devices. The solvent additive relatively affects the short-current density (J_{sc}) and fill factor (FF) of these devices without thermal annealing. The V_{oc} of devices gradually decreases with increasing DIO additive content. The devices with 0.25 vol% DIO have the highest PCE with V_{oc}, J_{sc}, FF, and PCE of 0.61 V, 8.96 mA/cm^2, 50.4%, and 2.73%, respectively. The devices processed with 0.5 vol% DIO exhibited a similar performance of devices with 0.25 vol% DIO. Noteworthy, the average PCE of devices was reduced from 2.46% to 2.11% as the DIO content increased from 0.5 to 1 vol%. According to our previous study,[17] the early stage of polymer crystallization during film drying process in the moving R2R step plays a critical role in the BHJ film morphology and device performance. Considering combinational

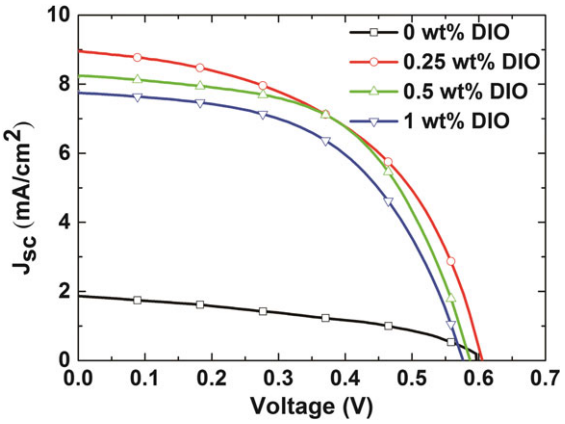

FIGURE 2 J-V curves of the P3HT:PC_{61}BM solar cells (cell area: 1 × 0.3 cm^2) prepared with various DIO contents and without additional thermal annealing [Colour figure can be viewed at wileyonlinelibrary.com]

TABLE 1 Performance of the P3HT:PC_{61}BM solar cells based on various DIO amounts without additional thermal annealing. The devices area is 0.3 cm^2 and the average PCEs are averaged over 15 devices

DIO Amount	J_{sc}, mA/cm^2	V_{oc}, V	FF, %	PCE, %	PCE_{ave}, %
0	1.87	0.61	41.5	0.48	0.38 ± 0.11
0.25	8.96	0.61	50.4	2.73	2.58 ± 0.08
0.5	8.44	0.59	54.3	2.70	2.46 ± 0.15
1	7.43	0.57	56.2	2.36	2.11 ± 0.19

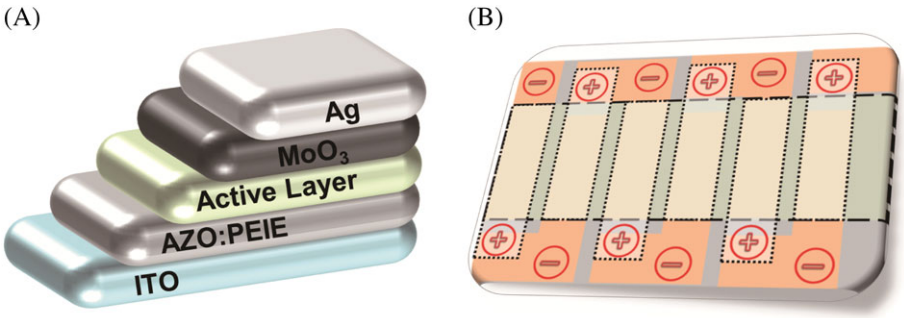

FIGURE 1 Schematic diagram of structure of (A) devices and (B) module. In the structure of the module, the cathode (marked in "−") is the etching ITO and the anode (marked in "+") is the thermally evaporated silver [Colour figure can be viewed at wileyonlinelibrary.com]

effect of drying temperature and additive, we increased the temperature of R2R oven from 110°C to 130°C and 150°C for each additive amount set at 0.25 and 0.5 vol%, respectively. Figure 3 shows the J-V curves of these slot-die–coated OPV devices (cell area: 1 × 0.3 cm^2), and the corresponding performances are listed in Table 2. These results show that the highest PCE tuned by the content of solvent additive varies with the R2R oven temperature. As the R2R oven temperature increases from 110°C to 130°C, the optimal solvent additive amount is shifted to 0.5 vol% from 0.25 vol%. Thus, the highest PCE achieves 3.1% from 2.63% mainly due to the increasing J_{sc}. Moreover, the same development trend of PCE was present as the R2R oven temperature was increased to 150°C. These results indicate that the PCE of additive-based devices manufactured by the R2R slot-die coating is also strongly influenced by the early stage of film formation from wet film to solid film. Therefore, we can further combine the use of solvent additive and R2R oven temperature to precisely control the film formation and thus optimize BHJ morphology.

To demonstrate the universal applicability of abovementioned R2R slot-die coating procedure for the LBG-polymer–based OPVs, we transferred this processing concept to the PTB7/$PC_{71}BM$ system that is known to perform high efficiency based on the conventional spin coat process. Several research groups have reported that the PCE of spin-coated PTB7:$PC_{71}BM$ OPVs achieved over 9%. To attain the commercialization target of OPV, a researcher group transferred the PTB7-Th–based OPV from spin coating under inert atmosphere to doctor-blade–coating under air environment.[40] The PCE of the PTB7-Th OPV on glass substrate fabricated under air was only 5.3%, but the performance can be improved to 8.3% by a posttreatment with alcohol-based solvent. Although the LBG-based OPVs have shown to be a promising potential to realize OPV commercialization, the PCE of flexible LBG-polymer–based devices manufactured by R2R mass production is still limited.[41] According to the previous results of the P3HT:$PC_{61}BM$:DIO devices, the combination of addition content of DIO and the R2R oven temperature could greatly influence the film

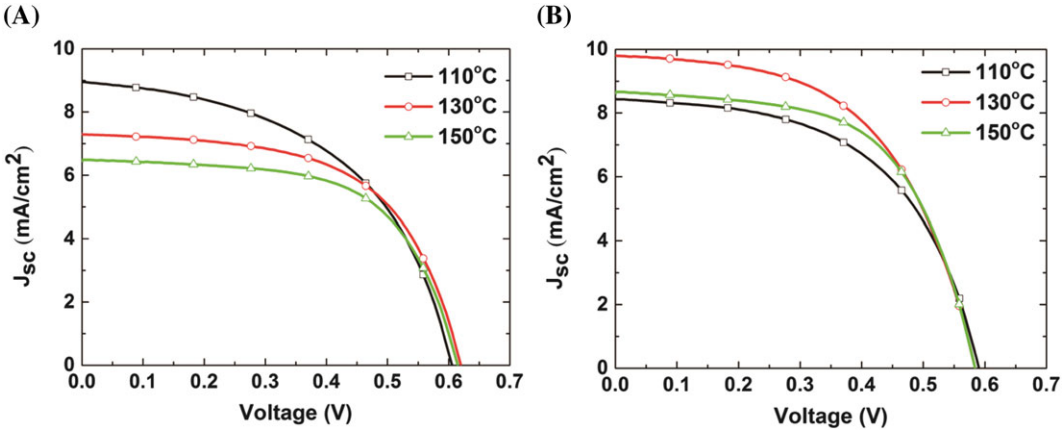

FIGURE 3 J-V curves of the P3HT:$PC_{61}BM$ solar cells (cell area: 1 × 0.3 cm^2) prepared with (A) 0.25 vol% and (B) 0.5 vol% of DIO under the R2R oven temperature of 110°C, 130°C, and 150°C [Colour figure can be viewed at wileyonlinelibrary.com]

TABLE 2 Performance of the P3HT:$PC_{61}BM$ solar cells with 0.25 and 0.5 vol% DIO amounts under various R2R oven temperatures. The devices area is 0.3 cm^2 and the average PCEs are averaged over 15 devices

DIO Amount	Oven Temp	J_{sc}, mA/cm^2	V_{oc} V	FF, %	PCE, %	PCE_{ave}, %
0.25	110	8.96	0.61	50.4	2.73	2.58 ± 0.08
	130	7.289	0.62	58.3	2.63	2.50 ± 0.12
	150	6.498	0.615	61.4	2.45	2.11 ± 0.28
0.5	110	8.44	0.59	54.3	2.70	2.46 ± 0.15
	130	9.809	0.583	54.2	3.10	3.04 ± 0.09
	150	8.677	0.584	59	2.99	2.8 ± 0.17

TABLE 3 Performance of the PTB7:$PC_{71}BM$ solar cells and module based on various DIO amounts with the R2R oven temperature of 130°C. The devices area are 0.3 and 2 cm^2, and the module area is 20 cm^2. The average PCEs of single cells and modules are averaged over 15 devices and 5 devices, respectively

Device Area	DIO Amount	J_{sc}, mA/cm^2	V_{oc}, V	FF, %	PCE, %	PCE_{ave}, %
0.3	0.5	9.07	0.69	33.1	2.06	1.79 ± 0.42
	1	10.97	0.74	43.2	3.52	3.427 ± 0.11
	1.5	14.01	0.77	57.0	6.14	6.007 ± 0.13
	2	15.91	0.76	60.3	7.32	6.93 ± 0.44
	3	12.24	0.76	53.9	5.02	4.68 ± 0.51
2	2	14.14	0.75	53.5	5.7	5.30 ± 0.57
Module	2	1.44	7.21	41.8	4.34	4.125 ± 0.24

formation and BHJ morphology on the flexible ITO/PET during the R2R slot-die process under air. These 2 effects are coupled herein. To obtain highly efficient R2R slot-die–coated OPVs, we firstly tuned the DIO addition content from 0.5 to 3 vol% for PTB7/PC_{71}BM system. Table 3 presents the overall photovoltaic performances of these PTB7:PC_{71}BM devices (cell area: 1 × 0.3 cm^2). Figure 4 plots the J-V curves of the corresponding devices under simulated AM 1.5G illumination (100 mW/cm^2). By increasing the DIO content from 0.5 to 1 vol%, the PCE of devices was improved from 1.79% to 3.43% because of the enhanced J_{sc} and FF. The PTB7/PC_{71}BM device with 2 vol% DIO successfully demonstrates a J_{sc} of 15.91 mA/cm^2, V_{oc} of 0.76 V, and FF of 60.3%, yielding a PCE of 7.32%. To the best of our knowledge, this is the highest efficiency that has been achieved so far in the reported flexible OPVs manufactured by R2R slot-die process under air. During the processing optimization, the additive DIO content is more critical to the variation of R2R oven temperature. The appropriate temperature of R2R oven in set at 130°C.

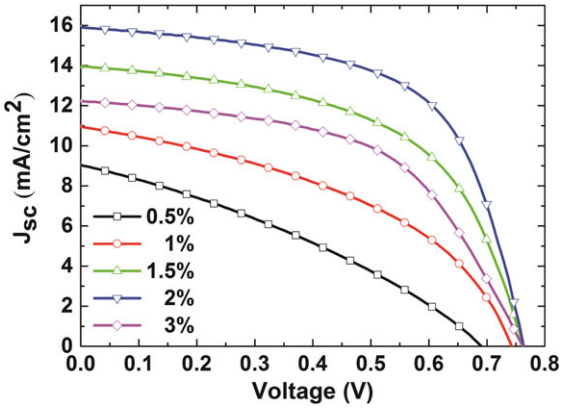

FIGURE 4 J-V curves of the PTB7:PC_{71}BM solar cells prepared with various DIO contents (cell area: 1 × 0.3 cm^2) [Colour figure can be viewed at wileyonlinelibrary.com]

To investigate the evolution of BHJ morphology of the R2R slot-die–coated films tailored by the DIO content and the R2R oven temperature, we have measured the morphology of these films by using AFM. Figure 5 shows the AFM images of BHJ morphology of P3HT:PC_{61}BM films with various DIO contents (0 and 0.5 vol%) and R2R oven temperatures (110°C, 130°C, and 150°C), respectively. Figure 5A was the morphology of the blend film without DIO under the R2R oven temperature of 110°C, and the root-mean-square (RMS) roughness determined by AFM was 1.4 nm. Although a

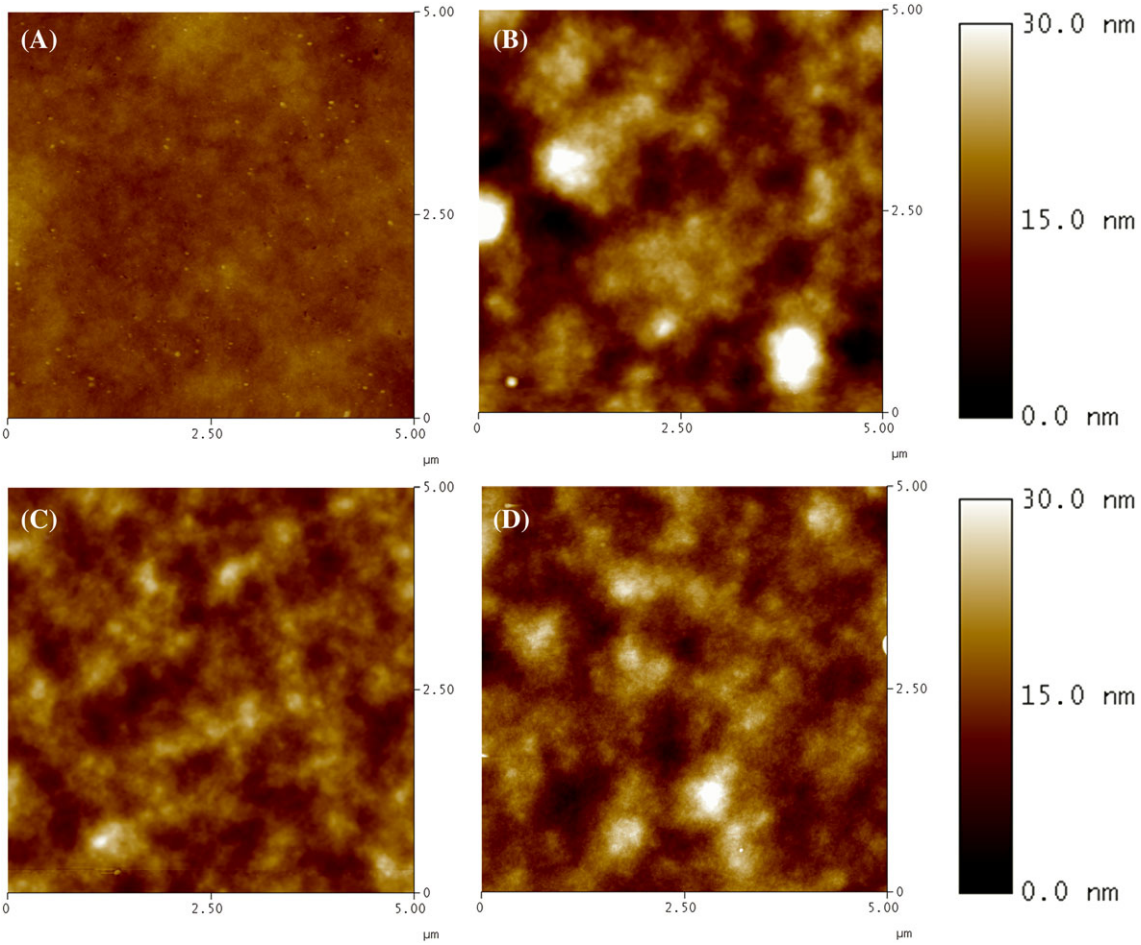

FIGURE 5 Atomic force microscopy images of the roll-to-roll slot-die–coated P3HT:PC_{61}BM films prepared with various DIO contents and at different roll-to-roll oven temperatures. A, pristine P3HT:PC_{61}BM film coated under roll-to-roll oven temperature of 110°C; B, P3HT:PC_{61}BM:0.5 vol% DIO film coated under roll-to-roll oven temperature of 110°C; C, P3HT:PC_{61}BM:0.5 vol% DIO film coated under roll-to-roll oven temperature of 130°C; and D, P3HT:PC_{61}BM:0.5 vol% DIO film coated under roll-to-roll oven temperature of 150°C [Colour figure can be viewed at wileyonlinelibrary.com]

smooth film was obtained under the coating condition, the R2R slot-die–coated film without DIO and thermal annealing presents a low PCE because of the insufficient charge transport paths resulted from the lack of suitable bicontinuous network of P3HT and $PC_{61}BM$ phases within the film. For the films prepared with 0.5 vol% DIO, they exhibit the well phase-separation between P3HT and $PC_{61}BM$ to form the effective BHJ structure with large domains into bicontinuous network (Figure 5B-D). According to our previous study,[17] the R2R oven temperature has an impact on the RMS roughness and P3HT crystallization of R2R slot-die–coated films. The similar morphological evolution was presented in the P3HT:$PC_{61}BM$ blend films prepared with the high-boiling-point additive. The films coated under the R2R oven temperature of 110°C, 130°C, and 150°C show the RMS roughness of 5.2, 3.0, and 3.9 nm, respectively. These results elucidate that the BHJ morphology of the R2R slot-die–coated films can be manipulated by varying the additive content and the R2R processing temperature. In comparison to the increase of polymer crystallinity, the control of hierarchically phase-separated BHJ morphology by additive has the critical effect on the PCE of OPVs.

Likewise, we applied this method to control the BHJ morphology of films consisting of PTB7 and $PC_{71}BM$. The solvent additive DIO greatly improved the performance of the devices based on PTB7:$PC_{71}BM$ blend film. The widely accepted reason for the performance improvement is that the DIO can reduce the nanoscale component domain size, thereby increasing interfacial area, exciton dissociation, and the associated photocurrent. Therefore, we focus on how the morphology of the PTB7:$PC_{71}BM$ films evolves with DIO contents of 1 and 2 vol%. Figure 6 shows the AFM images of the R2R slot-die–coated PTB7: $PC_{71}BM$ films with various DIO contents. It can be clearly observed from these images that there is a substantial difference in the film morphology. A large domain size representing the large-scale phase separation was clearly revealed in the film processed with 1 vol% DIO (Figure 6A). The large domains of phase separation lead to a poor efficiency of exciton dissociation. Upon addition of 2 vol% DIO, a significant reduction in the domain size represents the well mixing of phase separation, as shown in Figure 6B. In this case, which is different from the P3HT:$PC_{61}BM$ blend films, the marked increase of large interfacial area resulted from the fine domains plays an important role in the improvement of PCE.

Furthermore, we scale up the cell area to 1 × 2 cm^2. The PCE of PTB7/$PC_{71}BM$ device is reduced to 5.7% (J_{sc} = 14.1 mA/cm^2, V_{oc} = 0.75 V, FF = 53.5%). The reduction of PCE may be attributed to the coating uniformity and processing defects of active layer from the environment without good dust and humidity control, which can be improved in the future. The corresponding J-V curve is shown in Figure 7. Based on these solid processing parameters, we prepared a flexible module of active area 20 cm^2 (series and parallel connected 20 cells). The module PCE is 4.34% (J_{sc} = 1.44 mA/cm^2, V_{oc} = 7.21 V, FF = 41.8%), and the corresponding J-V curve is shown in Figure 8A. In addition, the stability of the module is shown in Figure 8B. The stability measurement was performed in the dark with ambient conditions tested according to ISOS-D-1 (shelf),[42] and the PCE was normalized to the corresponding initial value. The normalized PCE of the module maintains 92% of its original performance after 65 days. The stability of our OPV flexible module is comparable to that of PTB7:$PC_{71}BM$ devices on ITO/glass electrode.[43,44] This present study demonstrates the universal R2R slot-die coating approach for various polymers (P3HT ~ LBG polymer) with respect to the up-scaling from small high-PCE cell to large area module.

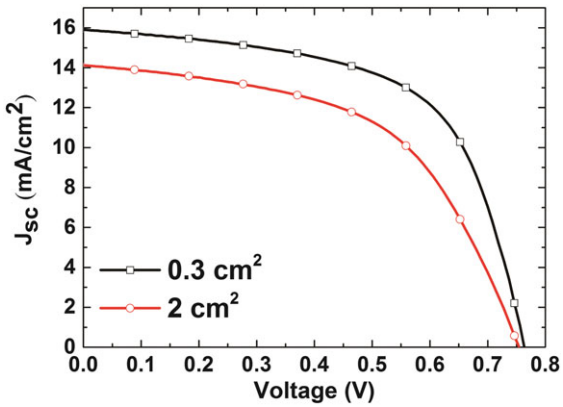

FIGURE 7 J-V curve of the PTB7:$PC_{71}BM$ solar cells with device area of 1 × 2 cm^2 [Colour figure can be viewed at wileyonlinelibrary.com]

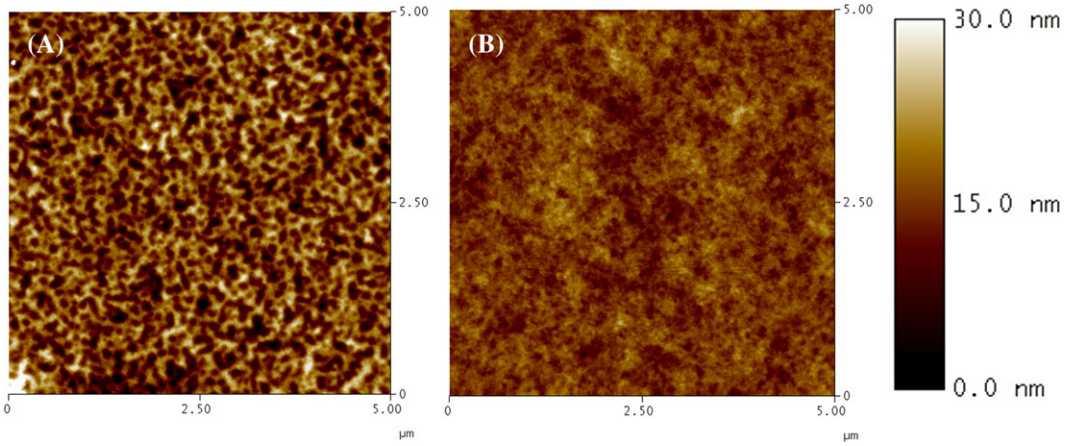

FIGURE 6 Atomic force microscopy images of the roll-to-roll slot-die–coated PTB7:$PC_{71}BM$ films prepared with various DIO contents of (A) 1 vol % and (B) 2 vol% [Colour figure can be viewed at wileyonlinelibrary.com]

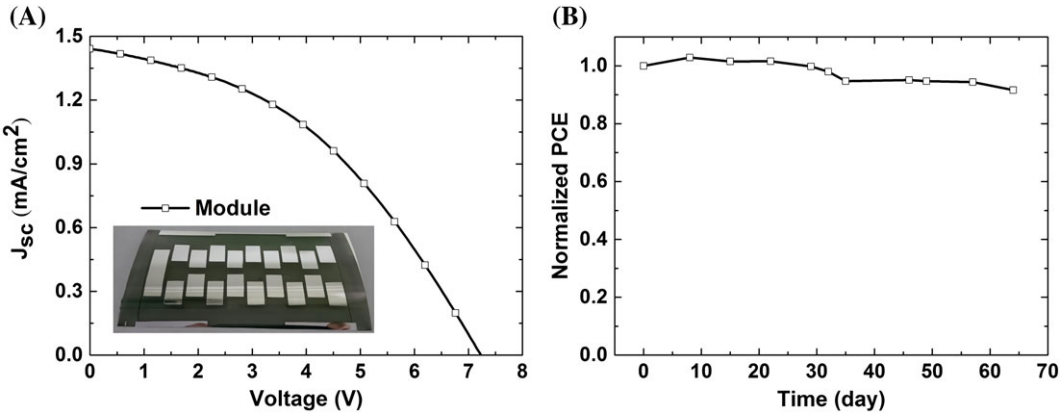

FIGURE 8 A, J-V curve and picture of the PTB7:$PC_{71}BM$ OPV module (1 × 1 cm^2 for each cell area). B, Normalized PCE of the encapsulated PTB7:$PC_{71}BM$ OPV module stored for 65 days in air under ambient conditions [Colour figure can be viewed at wileyonlinelibrary.com]

4 | CONCLUSIONS

We developed the facile R2R slot-die coating approach to significantly enhance the PCE of the flexible OPVs by combination of the additive and the R2R oven temperature universally for general polymers. The amount of DIO additive in the photoactive layer solution was used to significantly improve the performance by tailoring the nanomorphology and intermixing phase separation during the early stage of film formation during R2R oven drying. The highest PCE of 7.32% based on PTB7:$PC_{71}BM$:2%DIO is achieved using R2R slot-die coating process. Our study demonstrates a feasibility of solution-processable and environmental-friendly slot-die–coated high performance OPVs and the up-scaling to large area module.

REFERENCES

1. Darling SB, You F. The case for organic photovoltaics. *RSC Adv*. 2013;3(39):17633-17648.
2. Nian L, Gao K, Liu F, et al. 11% Efficient ternary organic solar cells with high composition tolerance via integrated near-IR sensitization and interface engineering. *Adv Mater*. 2016;28(37):8184-8190.
3. Kumari T, Lee SM, Kang S-H, Chen S, Yang C. Ternary solar cells with a mixed face-on and edge-on orientation enable an unprecedented efficiency of 12.1%. *Energ Environ Sci*. 2017;10:258-265.
4. Huang Y-C, Chia H-C, Chuang C-M, Tsao C-S, Chen C-Y, Su W-F. Facile hot solvent vapor annealing for high performance polymer solar cell using spray process. *Solar Energy Materials and Solar Cells* 2013; 114(0):24–30.
5. Eggenhuisen TM, Galagan Y, Coenen EWC, et al. Digital fabrication of organic solar cells by Inkjet printing using non-halogenated solvents. *Solar Energy Materials and Solar Cells* 2015; 134(0):364–372.
6. Galagan Y, Fledderus H, Gorter H, et al. Roll-to-roll slot-die coated organic photovoltaic (OPV) modules with high geometrical fill factors. *Energ Technol*. 2015;3(8):834-842.
7. Liu F, Ferdous S, Schaible E, et al. Fast printing and in situ morphology observation of organic photovoltaics using slot-die coating. *Adv Mater*. 2015;27(5):886-891.
8. Cha H-C, Huang Y-C, Hsu F-H, et al. Performance improvement of large-area roll-to-roll slot-die-coated inverted polymer solar cell by tailoring electron transport layer. *Solar Energy Materials and Solar Cells*. 2014;130:191-198.
9. Berny S, Blouin N, Distler A, et al. Solar trees: first large-scale demonstration of fully solution coated, semitransparent, flexible organic photovoltaic modules. *Advanced Science*. 2016;3(5): 1500342
10. Kim JH, Jung JW, Williams ST, Liu F, Russell TP, Jen AKY. Enhanced crystalline morphology of a ladder-type polymer bulk-heterojunction device by blade-coating. *Nanoscale*. 2015;7(25):10936-10939.
11. Ro HW, Downing J, Engmann S, et al. Morphology changes upon scaling a high efficiency, solution-processed solar cell from spin-coating to roll-to-roll coating. *Energ Environ Sci*. 2016;9:2835-2846.
12. Hong S, Kang H, Kim G, et al. A series connection architecture for large-area organic photovoltaic modules with a 7.5% module efficiency. *Nat Commun*. 2016;7:10279
13. Lucera L, Machui F, Kubis P, et al. Highly efficient, large area, roll coated flexible and rigid OPV modules with geometric fill factors up to 98.5% processed with commercially available materials. *Energ Environ Sci*. 2015;9:89-94.
14. Vak D, Hwang K, Faulks A, et al. 3D printer based slot-die coater as a lab-to-fab translation tool for solution-processed solar cells. *Advanced Energy Materials*. 2015;5(4): 1401539
15. Valimaki M, Apilo P, Po R, et al. R2R-printed inverted OPV modules—towards arbitrary patterned designs. *Nanoscale*. 2015;7(21):9570-9580.
16. Gu X, Zhou Y, Gu K, et al. Roll-to-roll printed large-area all-polymer solar cells with 5% efficiency based on a low crystallinity conjugated polymer blend. *Advanced Energy Materials*. 2017. https://doi.org/10.1002/aenm.201602742
17. Huang Y-C, Cha H-C, Chen C-Y, Tsao C-S. Morphological control and performance improvement of organic photovoltaic layer of roll-to-roll coated polymer solar cells. *Solar Energy Materials and Solar Cells*. 2016;150:10-18.
18. Liao H-C, Tsao C-S, Lin T-H, et al. Nanoparticle-tuned self-organization of a bulk heterojunction hybrid solar cell with enhanced performance. *ACS Nano*. 2012;6(2):1657-1666.
19. Huang Y-C, Tsao C-S, Chuang C-M, et al. Small- and wide-angle x-ray scattering characterization of bulk heterojunction polymer solar cells with different fullerene derivatives. *J Phys Chem C*. 2012;116(18):10238-10244.
20. Liao H-C, Tsao C-S, Shao Y-T, et al. Bi-hierarchical nanostructures of donor-acceptor copolymer and fullerene for high efficient bulk heterojunction solar cells. *Energ Environ Sci*. 2013;6:1938-1948.
21. Synooka O, Eberhardt K-R, Singh CR, et al. Influence of thermal annealing on pcdtbt:pcbm composition profiles. *Advanced Energy Materials*. 2013;4(5): 1300981
22. Chen H, Hsiao Y-C, Hu B, Dadmun M. Tuning the morphology and performance of low bandgap polymer: fullerene heterojunctions via solvent annealing in selective solvents. *Adv Funct Mater*. 2014;24(32):5129-5136.

23. Yao Y, Hou J, Xu Z, Li G, Yang Y. Effects of solvent mixtures on the nanoscale phase separation in polymer solar cells. *Adv Funct Mater*. 2008;18(12):1783-1789.
24. Schmidt-Hansberg B, Sanyal M, Grossiord N, et al. Investigation of non-halogenated solvent mixtures for high throughput fabrication of polymer–fullerene solar cells. *Solar Energy Materials and Solar Cells* 2012; 96(0):195–201.
25. Liao H-C, Ho C-C, Chang C-Y, Jao M-H, Darling SB, Su W-F. Additives for morphology control in high-efficiency organic solar cells. *Mater Today*. 2013;16(9):326-336.
26. Wang DH, Pron A, Leclerc M, Heeger AJ. Additive-free bulk-heterojuction solar cells with enhanced power conversion efficiency, comprising a newly designed selenophene-thienopyrrolodione copolymer. *Adv Funct Mater*. 2012;23(10):1297-1304.
27. Chu T-Y, Tsang S-W, Zhou J, et al. High-efficiency inverted solar cells based on a low bandgap polymer with excellent air stability. *Solar Energy Materials and Solar Cells*. 2012;96:155-159.
28. Fu G, Yang S, Shi J, et al. Formation of charge-transfer complexes significantly improves the performance of polymer solar cells based on PBDTTT-C-T: PC71BM. *Progress in Photovoltaics: Research and Applications*. 2014;23(6):783-792.
29. Zhao W, Ye L, Zhang S, Sun M, Hou J. A universal halogen-free solvent system for highly efficient polymer solar cells. *J Mater Chem A*. 2015;3(24):12723-12729.
30. Das S, Keum J, Browning J, et al. Correlating high power conversion efficiency of PTB7:PC71BM inverted organic solar cells to nanoscale structure. *Nanoscale*. 2015;7(38):15576-15583.
31. Zhao J, Zhao S, Xu Z, et al. Revealing the effect of additives with different solubility on the morphology and the donor crystalline structures of organic solar cells. *ACS Appl Mater Interfaces*. 2016;8(28):18231-18237.
32. Lou SJ, Szarko JM, Xu T, Yu L, Marks TJ, Chen LX. Effects of additives on the morphology of solution phase aggregates formed by active layer components of high-efficiency organic solar cells. *J Am Chem Soc*. 2011;133(51):20661-20663.
33. He Z, Zhong C, Su S, Xu M, Wu H, Cao Y. Enhanced power-conversion efficiency in polymer solar cells using an inverted device structure. *Nature Photonics*. 2012;6(6):591-595.
34. Yoon SM, Lou SJ, Loser S, et al. Fluorinated copper phthalocyanine nanowires for enhancing interfacial electron transport in organic solar cells. *Nano Lett*. 2012;12(12):6315-6321.
35. Lu L, Yu L. Understanding low bandgap polymer PTB7 and optimizing polymer solar cells based on it. *Adv Mater*. 2014;26:4413-4430.
36. Bottiger APL, Jorgensen M, Menzel A, Krebs FC, Andreasen JW. High-throughput roll-to-roll X-ray characterization of polymer solar cell active layers. *J Mater Chem*. 2012;22(42):22501-22509.
37. Zawacka NK, Andersen TR, Andreasen JW, et al. The influence of additives on the morphology and stability of roll-to-roll processed polymer solar cells studied through ex situ and in situ X-ray scattering. *J Mater Chem A*. 2014;2(43):18644-18654.
38. Liu K, Larsen-Olsen TT, Lin Y, et al. Roll-coating fabrication of flexible organic solar cells: comparison of fullerene and fullerene-free systems. *J Mater Chem A*. 2016;4(3):1044-1051.
39. Wan J, Fang G, Qin P, et al. The design and realization of large-scale patterned organic solar cells in series and parallel configurations. *Solar Energy Materials and Solar Cells*. 2012;101:289-294.
40. Li N, Brabec CJ. Air-processed polymer tandem solar cells with power conversion efficiency exceeding 10%. *Energ Environ Sci*. 2015;8:2902-2909.
41. Angmo D, Andersen TR, Bentzen JJ, et al. Roll-to-roll printed silver nanowire semitransparent electrodes for fully ambient solution-processed tandem polymer solar cells. *Adv Funct Mater*. 2015;25(28):4539-4547.
42. Reese MO, Gevorgyan SA, Jørgensen M, et al. Consensus stability testing protocols for organic photovoltaic materials and devices. *Solar Energy Materials and Solar Cells*. 2011;95(5):1253-1267.
43. Jia X, Jiang Z, Chen X, et al. Highly efficient and air stable inverted polymer solar cells using LiF-modified ITO cathode and MoO3/AgAl alloy anode. *ACS Appl Mater Interfaces*. 2016;8(6):3792-3799.
44. Arredondo B, Martín-López MB, Romero B, Vergaz R, Romero-Gomez P, Martorell J. Monitoring degradation mechanisms in PTB7:PC71BM photovoltaic cells by means of impedance spectroscopy. *Solar Energy Materials and Solar Cells*. 2016;144:422-428.

How to cite this article: Huang Y-C, Cha H-C, Chen C-Y, Tsao C-S. A universal roll-to-roll slot-die coating approach towards high-efficiency organic photovoltaics. *Prog Photovolt Res Appl*. 2017;25:928–935. https://doi.org/10.1002/pip.2907